Journal of Pressure Vessel Technology

Technical Brief

Design Strength of Primary Structural Welds in Free-Standing Structures

K. P. Singh,[1] A. I. Soler,[1] and S. Bhattacharya[2]

A rational analysis technique to evaluate structural integrity of primary welds in free-standing structures in accordance with the ASME Code is presented. This paper is intended to fill the void in the ASME Code rules for analyzing welds under "faulted" (level D) conditions in nonlinear free-standing structural components used in safety-related applications in nuclear power plants.

Nomenclature

d = distance of neutral axis from centerline (Fig. 5)
F_x, F_y, F_z = applied force loadings (Fig. 3)
M_x, M_y = applied moment loadings (Fig. 3)
M_L = limit moment
r_i = mean radius of ith weld ring
t_i = mean width (radial thickness) of ith weld ring
τ_F = force factor of safety
τ_M = moment factor of safety
τ_R = hybrid factor of safety
τ_s = shear factor of safety
θ_i = angular orientation of neutral axis with respect to weld line i
σ_i = "maximum stress" for ith weld patch

1 Background

With perhaps the sole exception of spent fuel storage racks, all equipment, components and appurtenances in nuclear power plants are firmly anchored to appropriate foundations. The early generation of fuel storage racks were also anchored structures. However, in the late 1970s U.S. nuclear power plants faced the prospect of indefinite onsite storage, and moved to retrofit existing fuel pools with racks which maximized the quantity of available storage. Existing fuel pool slabs could not be reconfigured to provide foundation anchors for the new replacement racks without great expense, disruption in plant operation, and a certain concern for safety of plant personnel. These considerations led the industry to adopt the so-called "free-standing" racks. These racks are essentially cellular structures with four or more support legs. Figure 1 shows the schematic of a rack module used in the Diablo Canyon Nuclear Power Plant of Pacific Gas and Electric Company. This rack, like all others, is designed to withstand seismic excitations stipulated for the power plant. The mathematical models and requirements of the analysis for this rack (and others) are governed by USNRC guidelines [1]. However, USNRC regulations are intended to provide a general framework, not a specific code for design. Specific criteria and design requirements are invoked by the USNRC documents by referring to other established sources, such as AISC Standards [2], and Subsection NF of the ASME Code, Section III [3]. For structural analysis and criteria, the analyst typically prefers the latter, which provides a rather complete set of criteria for structural qualification. Subsection "NF" has separate rules for three classes of structures, which are referred to as class 1, class 2 and class 3, respectively. The fuel racks have been designated as a class 3 structure.

Rules for class 3 structures in subsection "NF" of the code have provided a reasonably complete basis of structural qualification of racks. However, gaps in the code rules exist, pre-

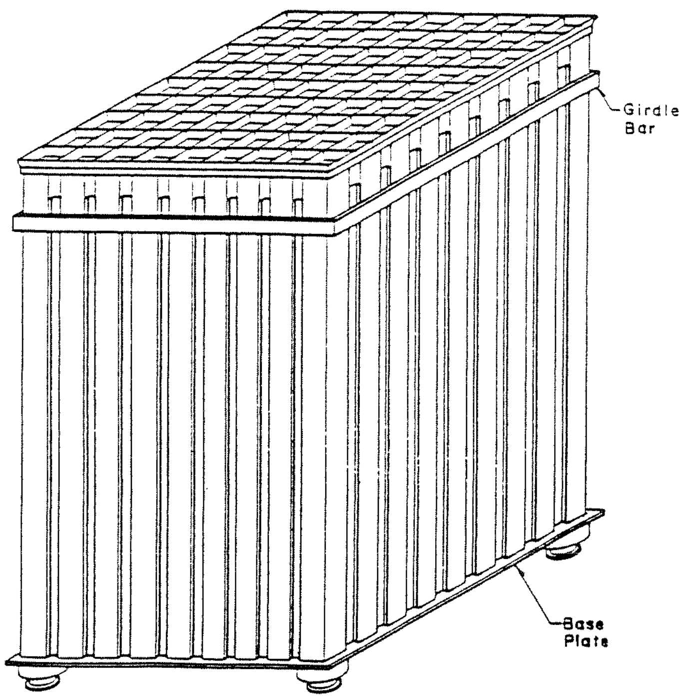

Fig. 1 Schematic of Diablo Canyon rack module

[1] Holtec International, Marlton, NJ 08053
[2] Pacific Gas and Electric Company, San Francisco, CA

Contributed by the Pressure Vessels and Piping Division, of THE AMERICAN SOCIETY OF MECHANICAL ENGINEERS. Manuscript received by the PVP Division, September 5, 1989; revised manuscript received March 22, 1991.

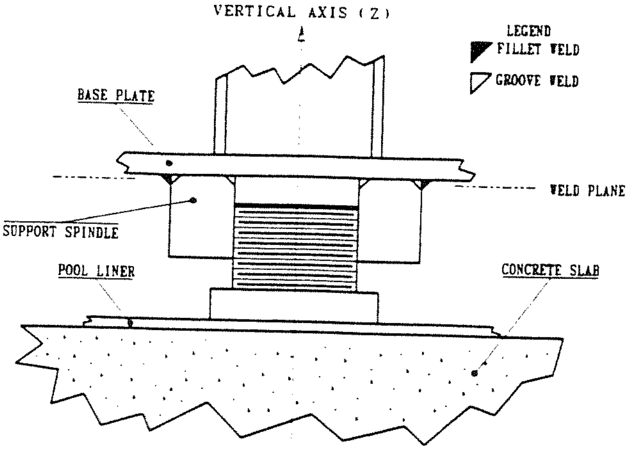

Fig. 2 Typical rack support geometry

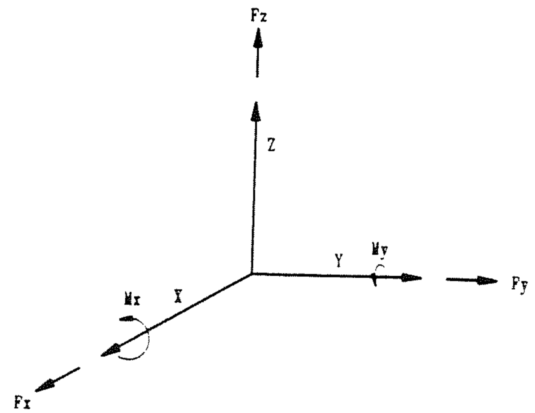

Fig. 3 Applied loadings at the support leg/base plate interface

sumably because "NF" rules [3] are contemplated for anchored structures, not for free-standing structures. The design criteria of "NF" [3], which we will hereinafter refer to as the "code," do not envisage short duration high amplitude loadings typical of free-standing structures undergoing rocking and sliding during a seismic event. The "NF" stress limits are focused on analyses performed by the response spectrum [4], or by static analysis techniques. Such analysis techniques are fundamentally inappropriate to analyze free-standing nonlinear structures. Aside from the nonlinearity introduced by lack of anchored connections between the rack and the foundation, similar lack of fixity between the fuel assemblies and storage cell makes the fuel rack structure a highly nonlinear one. Therefore, the seismic analysis of racks, of necessity, must be performed using one of the various time history integration techniques [6] which accurately captures high and low harmonics of the responses and provides the analyst with a complete time domain profile of the impact and impulse loads with all their sharp peaks and deep valleys.

A large portion of the peak load stems from "impact" effects and, as such, are strictly of very short duration. A stress analysis commensurate with the dynamic analysis would call for treating these impulsive loads using wave propagation theories. For class 3 structures, the Code [7] circumvents this necessity by posing stress limits on "primary" stresses only. In other words, the Code [7] limits the structural integrity assessment to ensuring that gross structural collapse will not occur. High local stresses, defined in the manner of the classical ASME Code for unfired pressure vessels [8], are considered accommodated by local plastic flows. In other words, when evaluating stress limit compliance, the stress field in the section under consideration is assumed to be fully developed and stress gradients due to St. Venant effects or stress concentrations are neglected. These fully developed section stresses, denoted as "primary stresses" are required to meet specific limits in direct tension, shear and flexure.

The foregoing concept for class 3 NF structures (such as the spent fuel racks) establishes a clear basis for assessment of structural integrity under design basis loads. The criteria, however, do not carry through in respect to "primary" structural welds, where further amplification of the design bases is required. However, in addition to the design basis loadings, there are other operational loads which also require structural evaluation. These are referred to level A (normal), level B (upset), level C (emergency), and level D (faulted) conditions in the Code [4]. Level D, the so-called faulted condition loading, arises from postulated events of extremely low probability, such as the safe shutdown earthquake. A nuclear structure is merely required to be safe from catastrophic failure or collapse under level D loadings; extensive structural yielding and deformation are acceptable. Subsection "NF" of the Code provides explicit stress limits on primary stresses under level D "conditions for linear members," but fails to provide specific rules for treating the welds which join such linear members to other portions of the structure. The weld joining the support legs to the base plate in Fig. 2, for example, is such a weld, which we will refer to as "primary welds." Recalling that the core requirement of the Code is that a total collapse of the structure does not occur, even as permanent deformation is permissible, it is possible to develop an NF-consistent procedure for analyzing primary welds subject to level D conditions. The purpose of this paper is to present the concepts evolved to develop such a procedure, and to articulate the concepts which underlie the proposed methodology. Much of the material presented herein was developed during authors' studies of the Diablo Canyon high-density racks in the period preceding the Atomic Safety Licensing Board hearings in 1986-1987.

2 Weld Configuration

A typical geometry of the primary structural welds in a spent fuel storage rack is illustrated in Fig. 2. An internally threaded support spindle is attached to the baseplate (Fig. 1) of the rack module through groove and fillet welds. Figure 2 shows the weld configuration utilized in the Diablo Canyon racks which, due to high seismicity of the central California coastal region, required large cross section welds. Considerations of warpage of the threads in the support spindle due to the heat of welding prompt the designers, where possible, to dispense with the internal groove welds, and minimize the size of other welds as well. However, the final weld configuration must provide sufficient structural connectivity to transfer the steady-state and dynamic reaction loads between the support legs and the body of the rack structure. During the seismic event, these reaction loads develop at the support leg/liner interface and are present only when the support pedestal is in contact with the fuel pool floor.

The reaction loads are primarily horizontal shear due to Coulomb friction between the support and the underbase structure (pool liner for racks) and vertical compression force due to dead load and the vertical motion of the rack leg (including impacts). These forces are equilibrated by five reaction loadings at the weld plane (Fig. 2). In Fig. 3 they are denoted as F_x, F_y, F_z, M_x and M_y. The object of this paper is to present a method to evaluate the design strength of the weld connection and to introduce the related concepts of "factor of safety" for different categories of seismic events. Details are presented here for pedestals of circular planform; the same design philosophy can be applied to pedestal weld planes of noncircular cross sections.

Table 1 Maximum tension and shear stresses for austenitic stainless steel at 150°F

Quantity	Value (ksi)	Reference ASME Code table
Ultimate strength (ksi)	68.1	Table I-3.2
Maximum tension stress (ksi) in partial penetration groove weld	42	Table NF-3324.5(a)-1 and Appendix F
Maximum shear stress (ksi)	28.6	Table NF-3523(b)-1 and Appendix F
Maximum tension or compression stress in fillet welds	28.6	———

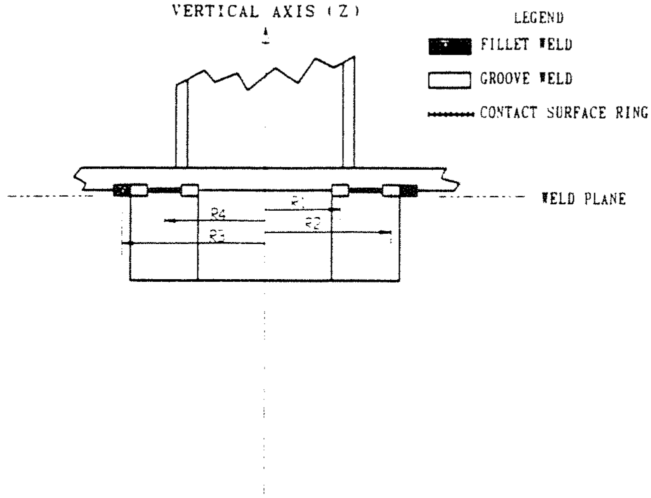

Fig. 4 Equivalent planar weld rings for Fig. 2 structure

3 Design Strength

The notion of design strength of welds has a direct parallel in the reinforced concrete literature [8]. In essence, the load-carrying capability of the structure is calculated by postulating that the "maximum stress" level is reached in the entire load-bearing region and that the stress distribution satisfies force and moment equilibrium. In this manner, the design strength moment and shear of a section are computed. To determine Code compliance, the analyst is required to increase the individual loading components by prescribed factors to obtain the factored load on the structure. For example, the multiplier on the operating basis earthquake is 1.25, and that on the safe shutdown earthquake is 1.0 [8]. The section moments and shears due to the factored load combinations are compared to their respective design strength values.

Similar load combinations are prescribed by the USNRC for "NF" structures as well [8]. It is, therefore, logical to develop a concept of design strength of a primary weld section along the lines of the parallel concept for reinforced concrete structures.

Although the reinforced concrete design code prescribes the ultimate strength of the re-bars as the "maximum stress," it need not be so for weld plane design strength evaluation. The logical and conservative value is the allowable Code stress corresponding to the so-called level D (faulted) condition of the ASME Codes. For example, the maximum stress values consistent with "NF" for a common austenitic stainless steel material—SA240-304L—are presented in Table 1.

To compute the design strength of the weld connection, the "maximum stress" is assumed to develop throughout the weld plane, although its sign may be tensile or compressive to satisfy moment and force equilibrium. The resulting stress distribution is of rectangular shape, akin to the fully developed plastic stress field in an elastic-perfectly plastic material. The stress distribution is characterized by a neutral axis. The location of the neutral axis, defined by its offset from the axis of symmetry and its angular orientation, depends on the applied direct loads and the two applied bending moments. However, for a given axial thrust, the maximum resultant moment M_L which would equilibrate the stress distribution corresponding to the design strength can be computed. Thus, a thrust-versus-moment "interaction curve" can be generated. This interaction curve quantifies the design strength of the weld plane. It is a derived physical property for the specified weld plane geometry and can be viewed as a limit which must be satisfied by the applied loads.

The foregoing discussion pertains to the interaction of direct and bending loads. Consistent with the spirit of "NF," the shear design strength is treated separately and no interaction analysis is done. The shear design strength is merely the gross shear which can be carried by the weld plane if the maximum shear stress is assumed to develop throughout the weld plane section. This practice of separate consideration of direct and shear stresses is the standard practice for class 3 components in Section III of the Code. On the other hand, equipment designed to higher classes of the ASME Code, such as class 1 components per subsection "NB," must deal with maximum "stress intensities," which involve combination of direct and shear stresses. It is felt that taking the minimum characteristic dimension, such as throat of the fillet weld, rather than its side dimension, to define the weld cross section introduces additional (desirable) conservatism in the evaluation of the design strength. We would, therefore, remain consistent with the provisions of the "NF" and treat shear and direct loads separately.

4 Formulation for Circular Sections

Before setting down the governing equations to evaluate the design strength, it is necessary to define the mathematical model for the weld connection. Consistent with the guidelines of the ASME Codes, the weld connection is simulated by planar rings of widths equal to the minimum characteristic dimension of the weld cross section. The weld planar rings for the circular support joint of Fig. 2 are illustrated in Fig. 4. The unwelded contact surface between the support leg and the baseplate is assumed to carry only compressive loads, and the "maximum" compressive stress on this interface is set equal to the tension and compression stress value of the adjoining groove weld.

A comment on the potential of metal-to-metal contact at the interface between the baseplate and support leg is warranted at this point. Fillet or groove welds of the type shown in Fig. 2 require addition of filler material during welding. The shrinkage of the weld puddle during cooling of the weld produces a tight metal-to-metal contact between the two welded parts. Such contact cannot be assured, for example, if the joining were done by electric resistance weld. However, electric resistance, or another type of nonfiller material weld, is not practical for this application. One can, in general, assume that a metal-to-metal contact at the support leg-base plate interface exists, unless the geometry of the welding detail is unusual, indicating the possibility of lack of such contact.

The welds in Fig. 2 are shown in the weld plane in Fig. 4. Radii r_i extend to the center of each weld annulus. The width of the weld rings is taken equal to the "throat" of the respective filled and groove welds.

To compute the design strength of a weld section in a support leg, it is necessary to specify an axial compression F_z and compute the associated limit moment M_L. The weld rings are modeled as thin rings of thickness t_i; and mean radii r_i (Fig. 5). Radii r_1, r_2, and r_3 denote the mean radii of the inner groove, the outer groove, and the fillet weld rings (Fig. 4), respectively. The fourth element is the spindle to baseplate interface (mean radius r_4). Element 4 is ineffective in tension, but can carry the compression load.

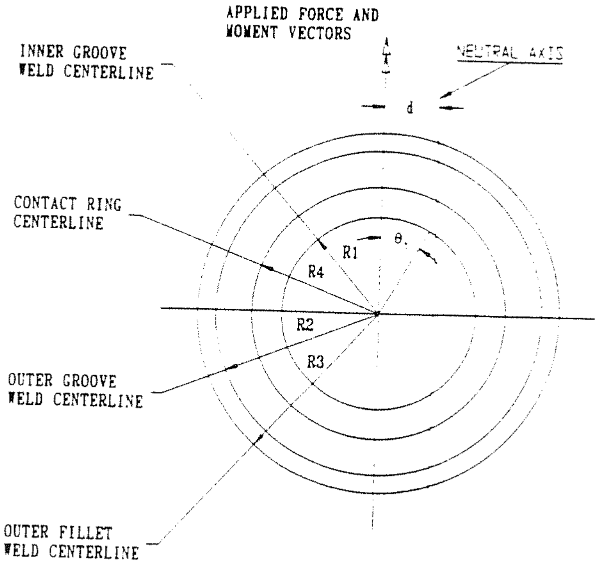

Fig. 5 Weld plane section and neutral axis

Figure 5 shows the centerlines of the four rings in the weld plane, and location of the neutral axis. Force equilibrium yields (Fig. 5)

$$F_z = \sum_{i=1}^{4} [(\pi + 2\theta_i)r_i t_i \sigma_i] - \sum_{i=1}^{3} (\pi - 2\theta_i)\sigma_i r_i t_i$$

or

$$F_z = 4\sum_{i=1}^{3} \theta_i r_i \sigma_i t_i + (\pi + 2\theta_4)\sigma_4 r_4 t_4 \qquad (1)$$

where

$$\theta_i = \sin^{-1}\frac{d}{r_i}; \quad i = 1, 2, 3, 4 \qquad (2)$$

For a given F_z d, the location of the neutral axis, can be computed using the *five* nonlinear relations expressed by Eqs. (1) and (2).

Moment Equilibrium. Taking moments about the centroidal axis, we have, after some algebra,

$$\sum_{1}^{4} 2\,\sigma_i r_i^2 t_i \cos\theta_i + \sum_{1}^{3} 2\sigma_i r_i^2\, t_i \cos\theta_i = M_L$$

or

$$4\sum_{1}^{3} \sigma_i r_i^2\, t_i \cos\theta_i + 2\sigma_4 r_4^2\, t_4 \cos\theta_4 = M_L \qquad (3)$$

where $\cos\theta_i = \cos\left(\sin^{-1}\frac{d}{r_i}\right)$

For a series of values of F_z, the corresponding limit moment M_L can be computed using Eq. (3) and a force/limit moment interaction curve for the section can be generated. This is best illustrated by considering a numerical example.

For illustration purposes we use the design and load data for the Diablo Canyon fuel racks. Table 2 gives the weld geometry. The following instantaneous peak reaction loads were obtained from time history analysis of the racks under a faulted condition load case:

Resultant lateral shear:	226 kips
Axial thrust, F_z:	290 kips
Resultant bending moment (vectorial sum of two orthogonal moments)	1294 kip-in.

Table 2 Weld data for the example problem

Weld line	Minimum characteristic dimension or throat (in.)	Effective radius (in.)	Shear area (in^2)
1 Interior groove	0.442	3.33	9.25
2 Exterior groove	0.442	4.29	11.91
3 Exterior fillet	0.442	4.71	13.08

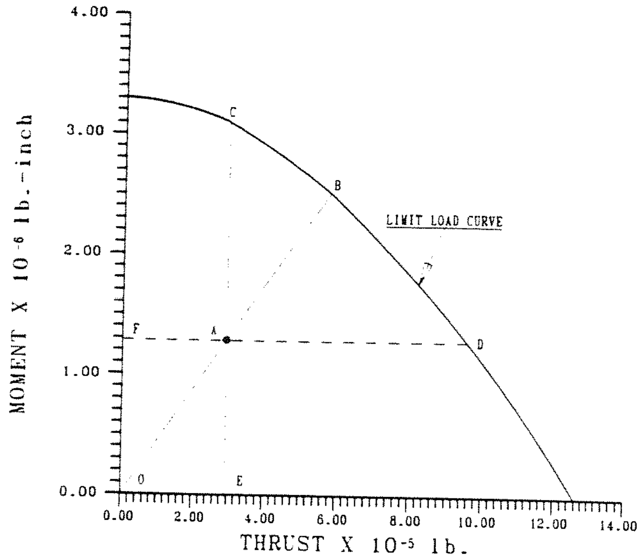

Fig. 6 Thrust/moment interaction curve

Figure 6 shows the thrust/moment interaction curve obtained for this geometry by solving Eqs. (1)-(3). The actual load point corresponding to the foregoing data is denoted as point A in Fig. 6. The factor of safety can be defined in three distinct ways:

(*a*) moment factor of safety, τ_M; ratio of limit moment to applied moment for a given compression load, i.e., EC/EA in Fig. 6;
(*b*) force factor-of-safety, τ_F; ratio of limit thrust to actual thrust for a given applied moment; i.e., FD/FA in Fig. 6;
(*c*) hybrid factor-of-safety, τ_R; ratio of OB to OA in Fig. 6.

In numerical computations, it is most convenient to compute τ_M since M_L is easily compared with the problem input $[M_1^2 + M_2^2]^{1/2}$ where M_1, M_2 are the reaction moments about two orthogonal axes with origin at the center of the pedestal.

The load point must lie inside of the interaction curve for level D loading condition. The Code prescribes a factor of 2.0 for austenitic stainless material (Appendix F of Section III) between stresses due to level D and level C loadings. Therefore, for level B or C condition (operating basis earthquake), at least one of the foregoing safety factors must exceed 2.0 in order to account for the lower limits that apply to these load levels. For the example problem, the ratio OB/OA $= \tau_R$ is equal to 1.92.

The shear load-carrying capability is readily calculated separately by multiplying the maximum shear stress by the effective weld ring areas. The shear factor of safety is simply the ratio of this limit shear load and the actual (applied) net shear load. Referring to Table 2, the total weld plane area is 34.24 sq. in. This leads to a shear design strength factor of safety τ_s = (34.24)(28.6)/226 = 4.33.

5 Closure

A computational procedure for evaluating the design strength of primary structural welds has been proposed. The method of analysis is consistent with the spirit of the ASME Code rules for component support structures, and bridges the disconnect in the Code rules when they are applied to geometrically nonlinear (free-standing) structures. Although the analysis is presented in the context of annular weld patches, it can be directly extended to other shapes.

Acknowledgment

The authors are thankful to Mr. Hans Ashar of USNRC for his input during this work effort.

References

1 Grimes, R. K., "OT Position for Review and Acceptance of Spent Fuel Storage and Handling Applications," USNRC, Washington, D.C., 1978.

2 *Manual of Steel Construction*, American Institute of Steel Construction, Chicago, Ill., 1980.

3 ASME Boiler and Pressure Vessel Code, Section III, Subsection NF, ASME, New York, 1983, 1986.

4 ASME Boiler and Pressure Vessel Code, Section III, Subsection NCA, ASME, New York, 1983, 1986.

5 Singh, K. P., and Soler, A. I., *Mechanical Design of Heat Exchangers and Pressure Vessel Components*, Chap. 21, Arcturus Publishers, Cherry Hill, N.J., 1984.

6 Soler, A. I., and Singh, K. P., "Seismic Response of Free Standing Fuel Rack Constructions to 3-D Motions," *Nuclear Engineering and Design*, Vol. 80, 1984, pp. 315–329.

7 Bernstein, M. D., "Design Criteria for Boilers and Pressure Vessels in the USA," *Proceedings of the Fifth International Conference on Pressure Vessel Technology*, Beijing, China, 1988.

8 ASME Boiler and Pressure Vessel Code, Section VIII, Div. I, ASME, New York, 1986.

9 "NUREG 0800, Section 3.8.4," USNRC, Washington, D.C., 1980.